Polarizabilities of Rydberg states of Rb atoms with *n* up to 140

Zhangli Lai,[1,2] Shichao Zhang,[1] Qingdong Gou,[2] and Yong Li[1,*]
[1]*Department of Physics, Central China Normal University, Wuhan 430079, China*
[2]*College of Mathematics and Physics, Jinggangshan University, Ji'an 343009, China*

(Received 6 August 2018; published 6 November 2018)

Up to the present, although experimental studies about the polarizabilities of alkali-metal Rydberg atoms have involved the states with principal quantum numbers $n \leqslant 80$, theoretical calculations are limited to the states with $n \leqslant 50$. In this work, we calculate the scalar and tensor polarizabilities of the $nS_{1/2}$, $nP_{1/2,3/2}$, and $nD_{3/2,5/2}$ Rydberg states of Rb with principal quantum number n up to 140 employing a model potential and the B-spline expansion technique. We obtain the polarizabilities that are in good agreement with the existing theoretical and experimental data.

DOI: 10.1103/PhysRevA.98.052503

I. INTRODUCTION

The Rydberg state refers to the highly excited state with a large principal quantum number n. Such states have attractive properties including large size, long radiative lifetime, strong dipole-dipole interaction, and large polarizability [1]. The polarizability, the fundamental property of an atom, can be described as the response of the atom to an external electric field and plays a significant role in the collision process and many other aspects of research [2]. In addition, the accurate values of the polarizabilities can be used to verify the consistency of oscillator strengths and the behavior of the outer region of a wave function itself [3]. Therefore, many theoretical methods have been applied to the calculations of the polarizabilities [4,5].

We have known that sufficient progress has been made in the studies about the polarizabilities of rubidium highly excited Rydberg atoms both theoretically and experimentally [6–19]. First, the polarizability of the $6\,^2P_{3/2}$ Rydberg state of Rb has been measured and calculated by Khadjavi *et al.* [6]. Later on, experimental investigations of the polarizabilities with rubidium for the nS ($n = 15$–80) and nD ($n = 13$–55) states were performed [12,13], and accurately calculated by Wijngaarden [14] for Rb nS and nD Rydberg states with $n \leqslant 13$ using the Coulomb approximation method [20]. Subsequently, several groups have calculated and measured polarizabilities of Rb Rydberg states with low n [5,16,19]. Recently, calculations of the polarizabilities of rubidium nS, $nP_{1/2,3/2}$, and $nD_{3/2,5/2}$ Rydberg atoms with $n = 8$–50 were made by Yerokhin *et al.* [18] using one-electron approximation and they also presented the theoretical values obtained by using the Coulomb approximation, which are in good agreement with each other. Up to the present, although experimental studies about the polarizabilities of alkali-metal Rydberg states have involved states with relatively high principal quantum numbers $n \leqslant 80$ [12,13], theoretical calculations have mainly involved the states with $n \leqslant 50$ [18]. Hence, it is interesting to extend the range of n from 50 to 80 for the theoretical calculations of the polarizabilities of alkali-metal Rydberg atoms. Actually, we calculate the polarizabilities of Rb with principal quantum number n up to 140 in this work.

The aim of the present work is to overcome the difficulties of the traditional Coulomb approximation [20] in calculating the radial matrix elements of the high Rydberg states of alkali-metal atoms and to use the model potentials and the B-spline expansion technique to calculate the radial matrix elements with the principal quantum number n up to 145. The obtained results are then used to calculate the polarizabilities of the nS, $nP_{1/2,3/2}$, and $nD_{3/2,5/2}$ Rydberg states of Rb with $n \leqslant 140$. The remainder of the paper is organized as follows. The general theory describing the scalar a_0 and tensor a_2 polarizabilities of a state (n, l, j) of Rb, the theoretical methods including the B-spline expansion technique, a parametric model potential, and quantum defect energies are presented in Sec. II. In Sec. III, the obtained results of the numerical calculations of the polarizabilities of the nS, $nP_{1/2,3/2}$, and $nD_{3/2,5/2}$ states of the Rb are presented and compared with the available theoretical and experimental values.

II. METHOD

A. Atomic polarizabilities

In term of the theory of the quadratic Stark effect, the scalar a_0 and tensor a_2 polarizabilities of the Rydberg states are calculated by [6]

$$a_0 = -\frac{2}{3}\sum_{n'l'j'}(2j'+1)\begin{Bmatrix} l & j & 1/2 \\ j' & l' & 1 \end{Bmatrix}^2 l_> \frac{|\langle nl|r|n'l'\rangle|^2}{E(j)-E(j')}, \tag{1a}$$

$$a_2 = -2\left[\frac{10j(2j-1)(2j+1)}{3(j+1)(2j+3)}\right]^{1/2}\sum_{n'l'j'}(-1)^{j+j'}(2j'+1)l_>,$$

$$\times\begin{Bmatrix} l & j & 1/2 \\ j' & l' & 1 \end{Bmatrix}^2\begin{Bmatrix} j & j' & 1 \\ 1 & 2 & j \end{Bmatrix}\frac{|\langle nl|r|n'l'\rangle|^2}{E(j)-E(j')}, \tag{1b}$$

---

[*] yongli@mail.ccnu.edu.cn

2469-9926/2018/98(5)/052503(8)

TABLE I. The parameters for the l-dependent model potential of the Rb.

Rb	a_1	a_2	a_3	a_4	r_c	α_c
$l = 0$	3.69628474	1.64915255	−9.86069196	0.19579987	1.66242117	9.0760
$l = 1$	4.44088978	1.92828831	−16.79597770	−0.81633314	1.50195124	
$l = 2$	3.7817363	1.57027864	−11.65588970	0.52942835	4.86851938	
$l \geqslant 3$	2.39848933	1.76810544	−12.07106780	0.77256589	4.79831327	

where $l_>$ is the larger of l and l'. We can obtain the specific expressions of the scalar and tensor polarizabilities of the nS, nP, and nD states as follows:

$$a_0(nS_{1/2}) = -\tfrac{1}{3}\left[\tfrac{4}{3}P(3/2) + \tfrac{2}{3}P(1/2)\right], \tag{2a}$$

$$a_0(nP_{1/2}) = -\tfrac{1}{9}[4D(3/2) + 2S(1/2)], \tag{2b}$$

$$a_0(nP_{3/2}) = -\tfrac{2}{5}D(5/2) - \tfrac{2}{45}D(3/2) - \tfrac{2}{9}S(1/2), \tag{2c}$$

$$a_2(nP_{3/2}) = \tfrac{2}{25}D(5/2) - \tfrac{8}{225}D(3/2) + \tfrac{2}{9}S(1/2), \tag{2d}$$

$$a_0(nD_{3/2}) = -\tfrac{2}{45}[P(3/2) + 5P(1/2)] - \tfrac{2}{5}F(5/2), \tag{2e}$$

$$a_0(nD_{5/2}) = -\tfrac{1}{9}\left[\tfrac{12}{5}P(3/2) + \tfrac{6}{35}F(5/2) + \tfrac{24}{7}F(7/2)\right], \tag{2f}$$

$$a_2(nD_{3/2}) = \tfrac{2}{9}P(1/2) - \tfrac{8}{225}P(3/2) + \tfrac{2}{25}F(5/2), \tag{2g}$$

$$a_2(nD_{5/2}) = \tfrac{4}{15}P(3/2) - \tfrac{16}{735}F(5/2) + \tfrac{20}{147}F(7/2). \tag{2h}$$

The following abbreviated symbols are used in the equation:

$$O(j) = e^2 \sum_{n'} \frac{|\langle nl|r|n'l'\rangle|^2}{E(nlj) - E(n'l'j')}$$

$$\equiv e^2 \sum_{n'} \frac{\left|R_{n'l'}^{nl}\right|^2}{E(nlj) - E(n'l'j')}. \tag{3}$$

Here O denotes S, P, D, F corresponding to $l = 0$, 1, 2, 3, respectively; $E(nlj)$ and $E(n'l'j')$ are zero-field energies of the (nlj) states and the intermediate $(n'l'j')$ states, respectively. The energies of Rydberg levels [1] are expressed in terms of the effective quantum number, and $\langle nl|r|n'l'\rangle$ is a radial matrix element, whose calculation is also the focus of this paper.

The sum in Eq. (3) implies the summations in principle over all allowed discrete and continuum intermediate states. However, in the actual calculations, the summations can be truncated to include only neighboring intermediate states contributing to the polarizability. From Eq. (3), we know that the calculation of the scalar a_0 and tensor a_2 polarizabilities of the Rydberg states is reduced to the calculation of the energies and the radial matrix elements.

B. Model potential and *B*-spline expansion technique

The Hamiltonian in the absence of the field for an alkali-metal atom is given by (in atomic units)

$$\hat{H}_0 = -\tfrac{1}{2}\nabla^2 + V(r), \tag{4}$$

where the one-electron parametric model potential $V(r)$ developed by Marinescu *et al.* [21] is written as

$$V_l(r) = -\frac{Z_l(r)}{r} - \frac{a_c}{2r^4}\left[1 - e^{-(r/r_c)^6}\right], \tag{5}$$

where a_c is the static dipole polarizability, r_c is the cutoff radius, and the radial charge $Z_l(r)$ is expressed as

$$Z_l(r) = 1 + (z-1)e^{-a_1 r} - r(a_3 + a_4 r)e^{-a_2 r}, \tag{6}$$

where z is the nuclear charge of the neutral atom. Obviously, the potential in Eq. (5) is l dependent. The optimized parameters $(a_1, a_2, a_3, a_4, r_c, a_c)$, as shown in Table I, are taken from Ref. [21].

The wave function of the Hamiltonian (4) in a zero field can be written as

$$\psi_{n,l,m}(r) = \frac{R_{n,l}(r)}{r} Y_l^m(\theta, \phi), \tag{7}$$

where $Y_l^m(\theta, \phi)$ is a spherical harmonic function and $R_{n,l}(r)$ is the radial wave function.

Substituting $V_l(r)$ and $\psi_{n,l,m}(r)$ into the Schrödinger equation of the Hamiltonian (4), we can obtain

$$\left[-\frac{d^2}{2dr^2} + \frac{l(l+1)}{2r^2} + V(r)\right]R_{n,l}(r) = E_{n,l}R_{n,l}(r). \tag{8}$$

In our calculations, using the B splines as a basis set [22,23], the radial wave function $R_{n,l}(r)$ can be expanded as

TABLE II. The parameters in Eqs. (11) and (12).

Level	R^* (cm^{-1})	E_∞ (cm^{-1})	δ_0	δ_2	Reference
$n\,^2S_{1/2}$	109736.623	33690.94644(1)	3.1311807(8)	0.1787 (2)	[25]
$n\,^2P_{1/2}$			2.6548849(10)	0.2900 (6)	[27]
$n\,^2P_{3/2}$			2.6416737(10)	0.2950 (7)	[27]
$n\,^2D_{3/2}$			1.3480948(11)	−0.6054(4)	[25]
$n\,^2D_{5/2}$			1.3464622(11)	−0.5940(4)	[25]
$n\,^2F_{5/2}$			0.0165192(9)	−0.085 (9)	[26]
$n\,^2F_{7/2}$			0.0165437(7)	−0.086 (7)	[26]

TABLE III. Comparison of the contributions to polarizability under the conditions of $|n–n'| \leqslant 2$ and $|n–n'| \leqslant 5$. For each n, the upper line represents the calculated polarizabilities under the condition of $|n–n'| \leqslant 2$, whereas the lower line represents the polarizabilities under the condition of $|n–n'| \leqslant 5$. All values are given in Hz/(V/cm)^2. $a[b]$ indicates $a \times 10^b$.

n	$a_0^{1/2}$ (S)	$a_0^{1/2}$ (P)	$a_0^{3/2}$ (P)	$a_0^{3/2}$ (D)	$a_0^{5/2}$ (D)	$a_2^{3/2}$ (P)	$a_2^{3/2}$ (D)	$a_2^{5/2}$ (D)
15	8.10[3]	2.91[4]	3.08[4]	2.11[4]	2.02[4]	−3.11[3]	9.48[3]	1.52[4]
	8.10[3]	2.91[4]	3.07[4]	2.12[4]	2.03[4]	−3.12[3]	9.38[3]	1.51[4]
25	3.80[5]	1.71[6]	1.81[6]	7.07[5]	6.64[5]	−1.63[5]	5.23[5]	8.26[5]
	3.79[5]	1.70[6]	1.81[6]	7.08[5]	6.66[5]	−1.63[5]	5.19[5]	8.21[5]
45	2.50[7]	1.41[8]	1.49[8]	3.87[7]	3.55[7]	−1.23[7]	4.13[7]	6.48[7]
	2.49[7]	1.40[8]	1.49[8]	3.87[7]	3.55[7]	−1.23[7]	4.10[7]	6.45[7]
65	3.26[8]	2.06[9]	2.19[9]	4.76[8]	4.32[8]	−1.73[8]	5.94[8]	9.30[8]
	3.25[8]	2.05[9]	2.18[9]	4.74[8]	4.30[8]	−1.73[8]	5.91[8]	9.26[8]
85	2.10[9]	1.42[10]	1.51[10]	2.98[9]	2.69[9]	−1.18[9]	4.07[9]	6.37[9]
	2.09[9]	1.42[10]	1.51[10]	2.97[9]	2.67[9]	−1.17[9]	4.05[9]	6.34[9]
105	9.12[9]	6.47[10]	6.89[10]	1.27[9]	1.14[10]	−5.28[9]	1.84[10]	2.87[10]
	9.10[9]	6.45[10]	6.87[10]	1.26[9]	1.13[10]	−5.26[9]	1.83[10]	2.86[10]
125	3.06[10]	2.24[11]	2.39[11]	4.23[10]	3.77[10]	−1.81[10]	6.36[10]	9.94[10]
	3.05[10]	2.23[11]	2.38[11]	4.21[10]	3.75[10]	−1.80[10]	6.33[10]	9.90[10]
135	5.22[10]	3.88[11]	4.13[11]	7.20[10]	6.41[10]	−3.12[10]	1.09[11]	1.71[11]
	5.20[10]	3.86[11]	4.12[11]	7.16[10]	6.36[10]	−3.11[10]	1.09[11]	1.71[11]
140	6.72[10]	5.03[11]	5.35[11]	9.25[10]	8.23[10]	−4.04[10]	1.42[11]	2.22[11]
	6.69[10]	5.01[11]	5.33[11]	9.20[10]	8.17[10]	−4.03[10]	1.41[11]	2.21[11]

TABLE IV. Calculated polarizabilities $n\,^2S$ [in Hz/(V/cm)^2] of the Rb Rydberg states, a comparison with the experimental [12] and previous theoretical [18] results. "This work" represents our calculated values. "Expt. and "Calc." represent the experimental and the previous theoretical results, correspondingly. $a[b]$ indicates $a \times 10^b$.

Level n^2S	$a_0^{1/2}$ (Expt.)	$a_0^{1/2}$ (Calc.)	$a_0^{1/2}$ (This work)
15	7.93[3]	7.98[3]	8.10[3]
20	7.22[4]	7.19[4]	7.33[4]
25	3.74[5]	3.70[5]	3.79[5]
30	1.39[6]	1.38[6]	1.41[6]
35	4.20[6]	4.13[6]	4.24[6]
40	1.06[7]	1.06[7]	1.09[7]
45	2.49[7]	2.41[7]	2.49[7]
50	5.06[7]	5.06[7]	5.22[7]
55	9.64[7]		1.01[8]
60	1.71[8]		1.86[8]
63	2.49[8]		2.61[8]
65	3.18[8]		3.25[8]
67	3.80[8]		4.01[8]
70	5.34[8]		5.45[8]
75	8.02[8]		8.80[8]
80	1.34[9]		1.37[9]
85			2.09[9]
90			3.12[9]
95			4.54[9]
100			6.48[9]
105			9.10[9]
110			1.25[10]
115			1.71[10]
120			2.29[10]
125			3.05[10]
130			4.00[10]
135			5.20[10]
140			6.69[10]

$R_{n,l}(r) = \sum_{i=1}^{N} c_i^{nl} B_{i,k}(r)$. Here $B_{i,k}(r)$ is the ith B spline of order k. Substituting $R_{n,l}(r) = \sum_{i=1}^{N} c_i^{nl} B_{i,k}(r)$ into Eq. (8), one can obtain

$$\left[-\frac{1}{2}\frac{d^2}{dr^2} + \frac{l(l+1)}{2r^2} + V(r)\right]\sum_{i=1}^{N} c_i^n B_{i,k}(r) = E_n \sum_{i=1}^{N} c_i^n B_{i,k}(r). \tag{9}$$

Both sides of Eq. (9) are multiplied by $B_{j,k}(r)$ and integrated over r; then we can obtain the matrix equation

$$\bar{H}\bar{C} = E\bar{S}\bar{C}, \tag{10}$$

where $\bar{H}$ is the Hamiltonian matrix, and $\bar{S}$ is the overlap matrix of the B splines. E and $\bar{C}$ are the eigenvalues and eigenvectors, respectively. Hence, solving this generalized eigenvalue equation, we can obtain the radial wave functions and then the radial matrix elements $\langle nl|r|n'l'\rangle$.

Due to the good behavior of the B splines, these radial wave functions have the correct number of nodes and good convergence behaviors. The method described here for obtaining the radial matrix elements is suitable for any alkali-metal atom.

C. Quantum defect energies

Schrödinger introduced the quantum defect nearly a century ago [24]. Since then, the concept of the quantum defects has been widely used in atomic physics, mostly (but not only) for calculation with respect to the energy levels of the Rydberg atoms. The energies of the Rydberg levels [1] are expressed in terms of the effective quantum number $(n - \delta_{n,l,j})$ as

$$E_{n,l,j} = E_\infty - \frac{R^*}{(n - \delta_{n,l,j})^2}, \tag{11}$$

where R^* is the Rydberg constant, E_∞ is the ionization limit, and $\delta_{n,l,j}$ is the quantum defect of the *nlj* Rydberg states and can be approximated by the modified Rydberg-Ritz coefficients for sufficiently large n [25]:

$$\delta_{n,l,j} \approx \delta_0 + \frac{\delta_2}{(n - \delta_0)^2}. \tag{12}$$

The modified Rydberg-Ritz coefficients (δ_0, δ_2) of the $nS_{1/2}$, $nP_{1/2,3/2}$, $nD_{3/2,5/2}$, and $nF_{5/2,7/2}$ states; the ionization limit E_∞; and the Rydberg constant R^* for the Rb atoms, as summarized in Table II, are taken from Refs. [25–27]. Thus, we can calculate the energies by making use of Eqs. (11) and (12).

TABLE V. Calculated polarizabilities n^2P [in Hz/(V/cm)^2] of the Rb Rydberg states, a comparison with the previous theoretical results [18]. "This work" and "Calc." represent our calculated and the previous theoretical results, correspondingly. $a[b]$ indicates $a \times 10^b$.

Level $n\,^2P$	$a_0^{1/2}$ (Calc.)	$a_0^{1/2}$ (This work)	$a_0^{3/2}$ (Calc.)	$a_0^{3/2}$ (This work)	$a_2^{3/2}$ (Calc.)	$a_2^{3/2}$ (This work)
13	8.53[3]	8.66[3]	9.33[3]	9.16[3]	−1.03[3]	−0.97[3]
15	2.86[4]	2.91[4]	3.13[4]	3.07[4]	−3.33[3]	−3.12[3]
20	2.93[5]	2.99[5]	3.23[5]	3.17[5]	−3.23[4]	−2.99[4]
25	1.67[6]	1.70[6]	1.84[6]	1.81[6]	−1.76[5]	−1.63[5]
30	6.70[6]	6.85[6]	7.39[6]	7.28[6]	−6.89[5]	−6.36[5]
35	2.13[7]	2.18[7]	2.35[7]	2.32[7]	−2.15[6]	−1.98[6]
40	5.75[7]	5.89[7]	6.37[7]	6.26[7]	−5.72[6]	−5.24[6]
45	1.37[8]	1.40[8]	1.52[8]	1.49[8]	−1.34[7]	−1.23[7]
50	2.96[8]	3.04[8]	3.28[8]	3.24[8]	−2.88[7]	−2.64[7]
55		6.11[8]		6.49[8]		−5.24[7]
60		1.15[9]		1.22[9]		−9.78[7]
65		2.05[9]		2.18[9]		−1.73[8]
70		3.51[9]		3.73[9]		−2.94[8]
75		5.77[9]		6.14[9]		−4.82[8]
80		9.19[9]		9.78[9]		−7.63[8]
85		1.42[10]		1.51[10]		−1.17[9]
90		2.14[10]		2.28[10]		−1.76[9]
95		3.15[10]		3.35[10]		−2.58[9]
100		4.55[10]		4.84[10]		−3.72[9]
105		6.45[10]		6.87[10]		−5.26[9]
110		8.99[10]		9.58[10]		−7.32[9]
115		1.23[11]		1.31[11]		−1.00[10]
120		1.67[11]		1.78[11]		−1.35[10]
125		2.23[11]		2.38[11]		−1.80[10]
130		2.95[11]		3.15[11]		−2.38[10]
135		3.86[11]		4.12[11]		−3.11[10]
140		5.01[11]		5.33[11]		−4.03[10]

III. RESULTS AND DISCUSSIONS

Using the procedures mentioned above, the radial wave functions which are convergent in highly excited states with $n = 145$ and have the correct number of nodes are obtained. Then the radial matrix elements $\langle nl|r|n'l'\rangle$ of the n-l alkali-metal Rydberg states in Rb with the principal quantum number n up to 145 are calculated by direct numerical integration [28]. Previously, Song and Li calculated the radial matrix elements $\langle nl|r|n'l'\rangle$ with n up to 145 using the model potentials and the *B*-spline expansion technique described above [28]. The results from Ref. [28] showed that this method is reliable and effective.

In order to verify the contributions of the neighboring intermediate states to the polarizabilities of the (n, l, j) states, we carry out approximate calculations of polarizabilities using model potentials and the *B*-spline expansion technique, and compare the results calculated under the conditions of $|n–n'| \leqslant 2$ and $|n–n'| \leqslant 5$, respectively. Computed results are presented Table III. By comparison, we can see that the error between the two cases is in the range of 1%. In this paper, all of the following results are the approximate values computed under the condition of $|n–n'| \leqslant 5$.

For a given *S* state, only the intermediate *P* states contribute to the scalar polarizabilities, and more than 99% of the scalar polarizability is contributed by the neighboring intermediate states. The calculated scalar polarizabilities with n from 15 to 140 are listed in Table IV. To facilitate comparison, the available theoretical values [18] and experimental data [12] are also presented in Table IV. As can be seen from Table IV, there is good agreement with the existing theoretical values [18] and experimental data [12].

For the *P* states, only intermediate *S* and *D* states contribute to the scalar and tensor polarizabilities. Furthermore, more than 99% of the scalar and tensor polarizabilities are contributed by the mostly neighboring intermediate states with $n' = n \pm 2$. The scalar and tensor polarizabilities of the $nP_{1/2,3/2}$ Rydberg states with $n = 13 - 140$ for the Rb are summarized in Table V which compares our results with the theoretical values [18]. We can see that our values agree well with the theoretical values [18], and the deviation is less than 5% for all the states considered. For now, we have not found any available experimental data. Consequently, the calculations of such polarizabilities of highly excited $nP_{1/2}$ and $nP_{3/2}$ states of Rb with $13 \leqslant n \leqslant 140$ will provide excellent benchmark tests of the experimental measurement.

For a given *D* state, only intermediate *P* and *F* states can contribute to the scalar and tensor polarizabilities. The calculated results from the $n\,^2D$ states are shown in

TABLE VI. Calculated polarizabilities $n\,^2D_{3/2}$ [in Hz/(V/cm)^2] of the Rb Rydberg states, a comparison with the experimental [13] and previous theoretical [18] results. "This work" represents our calculated values. "Expt." and "Calc." represent the experimental and the previous theoretical results, correspondingly. $a[b]$ indicates $a \times 10^b$.

n	$a_0^{3/2}$ (Expt.)	$a_0^{3/2}$ (Calc.)	$a_0^{3/2}$ (This work)	$a_2^{3/2}$ (Expt.)	$a_2^{3/2}$ (Calc.)	$a_2^{3/2}$ (This work)
13	7.81[3]	7.81[3]	7.79[3]	2.69[3]	2.73[3]	2.85[3]
15	2.14[4]	2.13[4]	2.12[4]	8.80[3]	8.98[3]	9.38[3]
20	1.60[5]	1.56[5]	1.54[5]	8.90[4]	8.93[4]	9.32[4]
25	7.40[5]	7.24[5]	7.08[5]	5.00[5]	4.98[5]	5.19[5]
30	2.60[6]	2.51[6]	2.45[6]	1.95[6]	1.97[6]	2.05[6]
35	7.40[6]	7.19[6]	7.00[6]	6.20[6]	6.19[6]	6.47[6]
37	1.08[7]		1.02[7]	9.20[6]		9.76[6]
40	1.85[7]	1.78[7]	1.73[7]	1.60[7]	1.66[7]	1.73[7]
45	4.20[7]	3.98[7]	3.87[7]	3.90[7]	3.93[7]	4.10[7]
50	8.50[7]	8.18[7]	7.92[7]	8.20[7]	8.48[7]	8.85[7]
55	1.64[8]		1.51[8]	1.63[8]		1.76[8]
60			2.74[8]			3.32[8]
65			4.74[8]			5.91[8]
70			7.87[8]			1.00[9]
75			1.26[9]			1.65[9]
80			1.96[9]			2.62[9]
85			2.97[9]			4.05[9]
90			4.40[9]			6.10[9]
95			6.38[9]			8.98[9]
100			9.07[9]			1.29[10]
105			1.26[10]			1.83[10]
110			1.74[10]			2.55[10]
115			2.37[10]			3.50[10]
120			3.18[10]			4.74[10]
125			4.21[10]			6.33[10]
130			5.52[10]			8.37[10]
135			7.16[10]			1.09[11]
140			9.20[10]			1.41[11]

TABLE VII. Calculated polarizabilities $n\,^2D_{5/2}$ [in Hz/(V/cm)^2] of the Rb Rydberg states, a comparison with the experimental [13] and previous theoretical [18] results. "This work" represents our calculated values. "Expt." and "Calc." represent the experimental and the previous theoretical results, correspondingly. $a[b]$ indicates $a \times 10^b$.

n	$a_0^{5/2}$ (Expt.)	$a_0^{5/2}$ (Calc.)	$a_0^{5/2}$ (This work)	$a_2^{5/2}$ (Expt.)	$a_2^{5/2}$ (Calc.)	$a_2^{5/2}$ (This work)
13	7.04[3]	7.36[3]	7.50[3]	4.70[3]	4.75[3]	4.61[3]
15	1.98[4]	1.99[4]	2.03[4]	1.51[4]	1.54[4]	1.51[4]
20	1.45[5]	1.44[5]	1.46[5]	1.49[5]	1.50[5]	1.48[5]
25	6.60[5]	6.56[5]	6.66[5]	8.11[5]	8.33[5]	8.21[5]
30	2.33[6]	2.26[6]	2.28[6]	3.20[6]	3.28[6]	3.24[6]
35	6.29[6]	6.42[6]	6.49[6]	1.04[7]	1.03[7]	1.02[7]
37	9.60[6]		9.45[6]	1.53[7]		1.53[7]
40	1.67[7]	1.58[7]	1.60[7]	2.62[7]	2.76[7]	2.72[7]
45	3.80[7]	3.50[7]	3.55[7]	6.40[7]	6.54[7]	6.45[7]
50	7.20[7]	7.16[7]	7.25[7]	1.34[8]	1.40[8]	1.38[8]
55	1.39[8]		1.38[8]	2.55[8]		2.77[8]
60			2.49[8]			5.20[8]
65			4.30[8]			9.26[8]
70			7.12[8]			1.57[9]
75			1.14[9]			2.59[9]
80			1.77[9]			4.11[9]
85			2.67[9]			6.34[9]
90			3.95[9]			9.55[9]
95			5.72[9]			1.41[10]
100			8.13[9]			2.02[10]
105			1.13[10]			2.86[10]
110			1.56[10]			3.99[10]
115			2.11[10]			5.47[10]
120			2.83[10]			7.41[10]
125			3.75[10]			9.90[10]
130			4.91[10]			1.30[11]
135			6.36[10]			1.71[11]
140			8.17[10]			2.21[11]

Tables VI and VII. Our calculated results of the Rb Rydberg states are compared with the theoretical [18] and experimental [13] values, which are in good agreement with each other.

By a qualitative analysis, there is the strong n^7 dependence of the polarizabilities [1]. In order to demonstrate whether our calculated polarizability values of the Rydberg states are approximately proportional to n^7, we use the following formula to represent the relationship between polarizabilities and n for the best fit:

$$a = An^b, \tag{13}$$

where the A and b parameters, obtained from a numerical fit of the calculated values of the scalar a_0 and tensor a_2 polarizabilities for the $nS_{1/2}$, $nP_{1/2,3/2}$, and $nD_{3/2,5/2}$ states to Eq. (13), are summarized in Table VIII. The exponent b's obtained are all close to 7 for the cases of the $nS_{1/2}$, $nP_{1/2,3/2}$, and $nD_{3/2,5/2}$ states, which is the value expected. Figures 1(a) and 1(b) show a comparison between the theory and the fitting for the scalar $a_0(nD_{3/2})$ and tensor $a_2(nD_{5/2})$ polarizabilities, respectively. Good agreement between the theory and the fitting is observed. It is also clearly shown that there are smooth dependences of the scalar a_0 and tensor a_2 polarizabilities on the principal quantum number n from Fig. 1.

The approximate constant ratios for the D state were found by O'Sullivan [13] with $a_0(nD_{5/2})/a_0(nD_{3/2}) \simeq 0.78(4)$ and $a_2(nD_{3/2})/a_2(nD_{5/2}) \simeq 0.62(2)$. This rule of constant ratios can be explained from our fitting formula $a = An^b$. From Table VIII, we can see that the exponent b's of the $a_0(D_{3/2})$

TABLE VIII. Scaling coefficients A and b in Eq. (13).

	$a_0 S_{1/2}$	$a_0\,(P_{1/2})$	$a_0\,(P_{3/2})$	$a_0\,(D_{3/2})$	$a_0\,(D_{5/2})$	$a_2\,(P_{3/2})$	$a_2\,(D_{3/2})$	$a_2\,(D_{5/2})$
A	8.19[−5]	2.49[−4]	2.67[−4]	1.48[−4]	1.47[−4]	−2.52[−5]	8.82[−5]	1.27[−4]
b	6.94	7.13	7.13	6.89	6.87	7.08	7.08	7.09

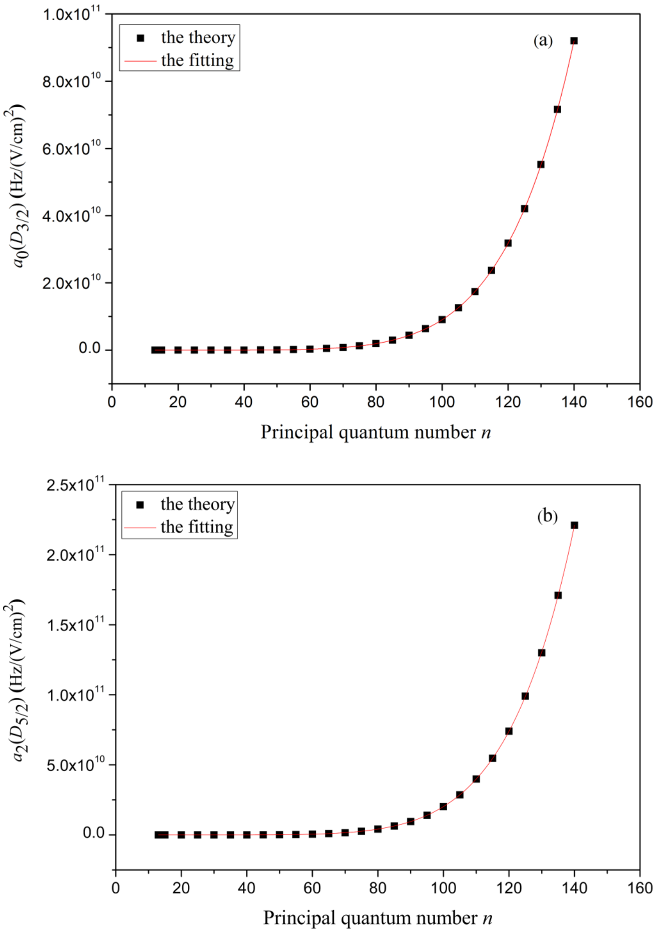

FIG. 1. (a) The scalar $a_0(D_{3/2})$ and (b) tensor $a_2(D_{5/2})$ polarizabilities. The squares are the calculated data. The solid represents the numerical fit of the polarizabilities to Eq. (13).

and $a_0(D_{5/2})$ are 6.89 and 6.87, respectively—almost the same. Therefore, we have

$$a_0(nD_{5/2})/a_0(nD_{3/2}) = \frac{1.47\times10^{-4}}{1.48\times10^{-4}}\frac{n^{6.87}}{n^{6.89}} \approx \frac{1.47\times10^{-4}}{1.48\times10^{-4}} = 0.99. \tag{14}$$

Similarly, for the ratio of the tensor polarizabilities we have

$$a_2(nD_{3/2})/a_2(nD_{5/2}) = \frac{8.82\times10^{-5}}{1.27\times10^{-4}}\frac{n^{7.08}}{n^{7.09}} \approx \frac{8.82\times10^{-5}}{1.27\times10^{-4}} = 0.69. \tag{15}$$

In addition to the constant ratios for the D state, we find that the constant ratio for the P state also holds; that is,

$$a_0(nP_{1/2})/a_0(nP_{3/2}) = \frac{2.49\times10^{-4}}{2.67\times10^{-4}}\frac{n^{7.13}}{n^{7.13}} = \frac{2.49\times10^{-4}}{2.67\times10^{-4}} = 0.93. \tag{16}$$

IV. SUMMARY

We have calculated the scalar and tensor polarizabilities of the $nS_{1/2}$, $nP_{1/2,3/2}$, and $nD_{3/2,5/2}$ Rydberg states of Rb with the principal quantum number n up to 140. In the numerical calculations, the employment of the B-spline expansion technique and the model potentials makes it feasible to obtain dipole transition matrix elements of the high Rydberg states. The results in this work are in good agreement with theoretical [18] and experimental values [12,13]. These studies provide in-depth understanding of the structure of atoms and molecules of highly excited Rydberg states.

ACKNOWLEDGMENT

We would like to thank Dr. Hongwei Song for much help.

[1] T. F. Gallagher, *Rydberg Atoms* (Cambridge University Press, Cambridge, 1994).
[2] T. M. Miller and B. Bederson, Adv. At. Mol. Phys. **13**, 1 (1978).
[3] B. Li, B. Liu, A. Chen, X. Zhang, and C. Zhang, J. Phys. B **21**, 2205 (1988).
[4] W. V. Wijngaarden, J. Quant. Spectrosc. Radiat. Transfer **52**, 555 (1994).
[5] M. S. Safronova and U. I. Safronova, Phys. Rev. A **83**, 052508 (2011).
[6] A. Khadjavi, A. Lurio, and W. Happer, Phys. Rev. **167**, 128 (1968).
[7] S. Svanberg, Phys. Scr. **5**, 132 (1972).
[8] W. D. Hall and J. C. Zorn, Phys. Rev. A **10**, 1141 (1974).
[9] R. W. Molof, H. L. Schwartz, T. M. Miller, and B. Bederson, Phys. Rev. A **10**, 1131 (1974).
[10] W. Hogervorst and S. Svanberg, Phys. Scr. **12**, 67 (1975).
[11] K. Fredriksson and S. Svanberg, Z. Phys. A **281**, 189 (1977).
[12] M. S. O'Sullivan and B. P. Stoicheff, Phys. Rev. A **31**, 2718 (1985).
[13] M. S. O'Sullivan and B. P. Stoicheff, Phys. Rev. A **33**, 1640 (1986).
[14] W. A. Van Wijngaarden, J. Quant. Spectrosc. Radiat. Transfer **57**, 275 (1997).
[15] A. Derevianko, W. R. Johnson, M. S. Safronova, and J. F. Babb, Phys. Rev. Lett. **82**, 3589 (1999).
[16] J. Walls, J. Clarke, S. Cauchi, G. Karkas, H. Chen, and W. A. van Wijngaarden, Eur. Phys. J. D **14**, 9 (2001).
[17] S. G. Porsev and A. Derevianko, J. Chem. Phys. **119**, 844 (2003).
[18] V. A. Yerokhin, S. Y. Buhmann, S. Fritzsche, and A. Surzhykov, Phys. Rev. A **94**, 032503 (2016).
[19] S. Snigirev, A. Golovizin, D. Tregubov, S. Pyatchenkov, D. Sukachev, A. Akimov, V. Sorokin, and N. Kolachevsky, Phys. Rev. A **89**, 012510 (2014).
[20] M. L. Zimmerman, M. G. Littman, M. M. Kash, and D. Kleppner, Phys. Rev. A **20**, 2251 (1979).
[21] M. Marinescu, H. R. Sadeghpour, and A. Dalgarno, Phys. Rev. A **49**, 982 (1994).
[22] C. de Boor, *A Practical Guide to Splines* (Springer, New York, 1978).
[23] H. Bachau, E. Cormier, P. Declev, J. E. Hansen, and F. Martin, Rep. Prog. Phys. **64**, 1815 (2001).

[24] D. R. Bates and A. Damgaard, Philos. Trans. R. Soc. London **242**, 101 (1949).

[25] M. Mack, F. Karlewski, H. Hattermann, S. Höckh, F. Jessen, D. Cano, and J. Fortágh, Phys. Rev. A **83**, 052515 (2011).

[26] J. Han, Y. Jamil, D. V. L. Norum, P. J. Tanner, and T. F. Gallagher, Phys. Rev. A **74**, 054502 (2006).

[27] W. Li, I. Mourachko, M. W. Noel, and T. F. Gallagher, Phys. Rev. A **67**, 052502 (2003).

[28] H. Song and Y. Li, Phys. Rev. A **78**, 062504 (2008).